J. Membrane Biol. 47, 377–399 (1979)

A Mathematical Model of Proximal Tubule Absorption

Ronald E. Huss and John L. Stephenson*

Section on Theoretical Biophysics, National Heart,
Lung and Blood Institute, and Mathematical Research Branch,
National Institute of Arthritis, Metabolism and Digestive Diseases,
National Institutes of Health, Bethesda, Maryland 20205

Received 30 August 1978; revised 16 February 1979

Summary. A previous model of the mechanisms of flow through epithelia was modified and extended to include hydrostatic and osmotic pressures in the cells and in the peritubular capillaries. The differential equations for flow and concentration in each region of the proximal tubule were derived. The equations were solved numerically by a finite difference method. The principal conclusions are: (i) Cell NaCl concentration remains essentially isotonic over the pressure variations considered; (ii) channel NaCl concentration varies only a few mosmol from isotonicity, and the hydrostatic and osmotic pressure differences across the cell wall are of the same order of magnitude; (iii) both reabsorbate osmolality and pressure-induced flow are relatively insensitive to the geometry of the system; (iv) a strong equilibrating mechanism exists in the sensitivity of the reabsorbate osmolality to luminal osmolality; this mechanism is far more significant than any other parameter change.

Glossary

A	Cross-sectional area, cm^2
α	Normalized flow, dimensionless
b	Solute concentration gradient osmol cm^{-4}
β	Slope of concentration of proximal tubule reabsorbate as a function of concentration difference between lumen and surrounding interstitium, dimensionless
C	Solute concentration osmol cm^{-3}
$\bar{C}$	Average membrane concentration of solute, osmol cm^{-3}
D_η	Diffusion coefficient, cm^2 sec^{-1}
δ_η	Dimensionless membrane parameter, 0 if variable, 1 if fixed
f	Fractional solute absorption from proximal tubule
$F_{s\eta}$	Axial solute flow, osmol sec^{-1} cm^{-1}
$F_{v\eta}$	Axial volume flow, cm^3 sec^{-1}
γ	Normalized solute concentration, dimensionless

* *Mailing address and to whom reprint requests should be made:* Chief, Section on Theoretical Biophysics, NHLBI, Bldg. 31, Room 4B44, National Institutes of Health, Rockville Pike, Bethesda, Maryland 20205.

0022-2631/79/0047-0377 $04.60

$H_{s\eta}$ Solute permeability, cm sec^{-1} (cm^3 sec^{-1} if area adjusted)
$J_{s\eta}$ Transmural solute flow, osmol sec^{-1} cm^{-1}
$J_{v\eta}$ Transmural volume flow, cm^2 sec^{-1}
L Total axial length, cm
$L_{p\eta}$ Hydraulic permeability, cm sec^{-1} $mmHg^{-1}$ (cm^3 sec^{-1} $mmHg^{-1}$ if area adjusted)
N Solute active transport rate, osmol cm^{-2} sec^{-1}
ξ Compliance parameter, $mmHg^{-1}$
P_η Hydraulic pressure, mmHg
P_{CAP} Sum of capillary hydrostatic and oncotic pressure, mmHg
P_I Sum of interstitial hydrostatic and oncotic pressure, mmHg
Π_η Protein oncotic pressure, mmHg
r Fraction of total cross-sectional area occupied by channel, dimensionless
r_{max} Limiting fractional area, dimensionless
R Universal gas constant, mmHg T^{-1} mol^{-1}
S Circumference, cm
σ Reflection coefficient, dimensionless
T Absolute temperature, °K
x Distance, cm
x' Normalized length, dimensionless

Subscripts $\eta = A, b, c, e, E, i, l, o, q, t$

A Absorbate
b Basement membrane
c Cell
e Channel
E Equilibrium between absorbate and lumen
i Interstitium
l Tubule lumen
o Isotonic
q Capillary
t Tight junction

It is well known that fluid reabsorption by the renal proximal tubule is powered by active transport of NaCl, and that the rate of reabsorption varies with the levels of hydrostatic and colloid oncotic pressure in the plasma of blood perfusing the peritubular capillaries [2–6, 9, 13, 18–20]. Experimental data show that this flow persists in the face of large negative pressure gradients across the tubule wall, thus ruling out a totally passive membrane model.

To account for these phenomena, attention was focused on the lateral intercellular channels as the site of transport activity [17, 23]. Tormey and Diamond concluded that these spaces provide a restricted region where solute concentration can build up, thus extracting water from the cell; with a blind end channel, such as these were postulated to be, the fluid would emerge into the interstitium, having attained equilibrium during its course down the channel. This process was modelled by Diamond and Bossert [8] who showed that the process was capable, in principle, of generating a nearly isotonic reabsorbate. However, since

hydrostatic pressure is not a variable in Diamond and Bossert's model, no test of pressure modulation of flows could be made.

Other recent evidence [1, 7, 9–12, 14, 19, 23] indicates that the tight junction may provide a pathway for a significant flow of solute into the channel. In an earlier paper [15], we presented a model of the channel, which included the tight junction, under the assumption that the cell is isotonic with respect to the luminal fluid and that the interstitial pressure is the same as the combined hydrostatic and protein oncotic pressures in the peritubular capillary lumen. Under these assumptions, we showed that a set of parameters could be selected such that an essentially isotonic fluid is delivered over a pressure range considered physiologically meaningful, and the modulating effect of pressure on flow is in agreement with experimental findings. Such a system requires a basement membrane of high solute and hydraulic permeabilities, and a tight junction having low hydraulic permeability but high solute permeability. The latter is required in order to provide the proper modulation.

It was also found that the hydrostatic pressure is a crucial variable in the system; although the pressures are low (on the order of 10 mmHg), they are sufficient to cause the channel to equilibrate at osmotic concentrations differing by less than 5 mosmol from isotonicity.

These numerical results demonstrated certain shortcomings in the assumptions. The finding that the channel concentration is very near isotonicity led us to look more closely at the cell as an element of the system, rather than simply as a bath, since even very small concentration differences could prove to be very significant. Another addition, suggested by the sensitivity to hydrostatic pressure, is the separation of the peritubular capillary from the interstitium.

In this paper, the original model is extended, principally by adding the cell as a reactive element of the system having a concentration gradient and a hydrostatic pressure separate from those of the tubule lumen. A second extension is the inclusion of the peritubular capillary as an additional element. The pressure in the interstitium is such that flow from the tubule exactly balances the capillary reabsorption.

The parameter sensitivity of this extended model was explored, and in general very closely paralleled that of the channel model previously reported. These studies are summarized briefly. In addition the model was used to investigate the dependence of the osmolality of the absorbate on that of the luminal fluid. It was found that this dependence dominated any parameter sensitivity by orders of magnitude. The slope characteris-

tic is such that tubular fluid and reabsorbate equilibrate in a small fraction of proximal tubule length at quasi-isotonicity.[1]

Derivation of Model Equations

The differential equations of the model are derived from flow concentration relations along the channel and cell, and across the bounding membranes. Figure 1 shows our representation of a section of tubule wall.

The cell walls are assumed to be compliant and their positions determined by the hydrostatic pressure difference between channel and cell. Solute moves into the channel through the lateral cell walls via active pumps located along the walls, and also by passive diffusive flow.

Consider a short segment of channel between x and $x+\Delta x$; if $F_{ve}(x)$ is the total axial volume flow at x, then the difference between $F_{ve}(x+\Delta x)$ and $F_{ve}(x)$ is the rate of fluid flow through the wall segment, which we denote by $J_{ve}(x)\Delta x$ with the sign convention that $J_{ve}(x)$ is positive if volume flow is from channel to cell. Standard analytic techniques yield the differential equation for conservation of volume flow

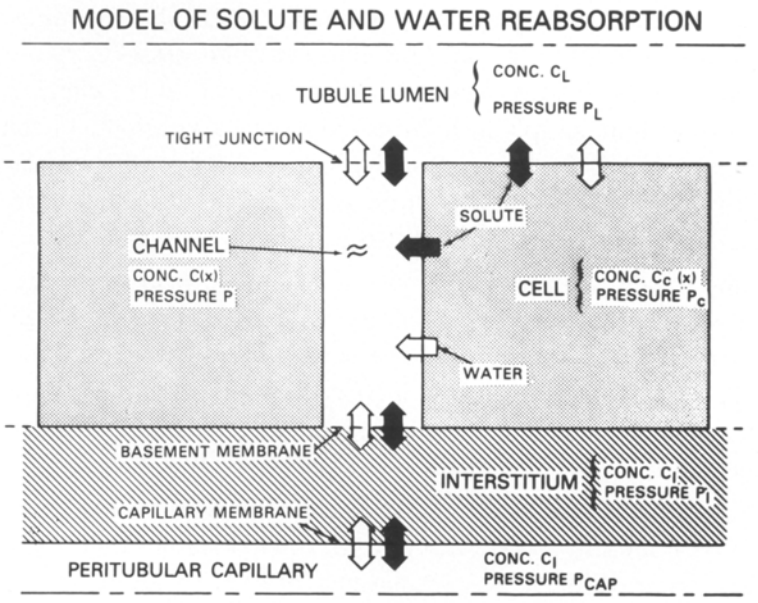

Fig. 1. Representation of section of tubule wall

[1] A preliminary report of this work was given previously [16].

$$\frac{dF_{ve}}{dx} = -J_{ve}. \tag{1}$$

We have a similar equation for conservation of total axial solute flow F_{se}

$$\frac{dF_{se}}{dx} = -J_{se}, \tag{2}$$

where J_{se} is transmural solute flux from channel to cell. Axial solute flow is the sum of a convective and diffusive term, or

$$F_{se} = F_{ve}\, C_e - D_e\, A_e \frac{dC_e}{dx} \tag{3}$$

where C_e is solute concentration in the channel, D_e is the diffusion coefficient in the channel and A_e is the cross-sectional area of the channel.

A set of equations, identical except for subscripting, describe solute and volume flow in the cell, namely

$$\frac{dF_{vc}}{dx} = -J_{vc}, \tag{4}$$

$$\frac{dF_{sc}}{dx} = -J_{sc} \tag{5}$$

and

$$F_{sc} = F_{vc}\, C_c - D_c\, A_c \frac{dC_c}{dx}. \tag{6}$$

We note that by definition

$$J_{ve} \equiv -J_{vc} \equiv J_v \tag{7}$$

and

$$J_{se} \equiv -J_{sc} \equiv J_s. \tag{8}$$

The transmural volume flow is given by

$$J_{ve} = S(x)\, L_{pe}[P_e(x) - P_c(x) + \sigma_e RT(C_c(x) - C_e(x))] \tag{9}$$

where L_{pe} is the hydraulic permeability of the wall separating cell and channel, $S(x)$ is its circumference, $P_e(x) - P_c(x)$ is hydrostatic pressure difference between channel and cell, σ_e is the Staverman reflection coefficient, R is the gas constant, and T is the absolute temperature. We assume that the solute is a neutral salt and that both the cell and the channel are well-mixed radially.

Transmural solute flow is given by

$$J_{se}(x) = -N(x) + (1-\sigma_e)\, J_{ve}(x) \left[\frac{C_e(x) + C_c(x)}{2}\right] - S(x)\, H_{se}[C_c(x) - C_e(x)] \tag{10}$$

where $N(x)$ is the rate of solute pumping into the channel. Solvent drag provides the second term of Eq. (10). The concentrations on both sides of the membrane are sufficiently close to each other so that in this term the arithmetic mean can be used for the average concentration. Diffusion across the walls provides the final term of Eq. (10), where H_{se} is the solute permeability measured in $\text{cm} \cdot \text{sec}^{-1}$.

An estimate of the pressure drop over the length of the channel was made by assuming a Hagen-Poiseuille relationship, and assuming also that the channel was of circular cross-section. The pressure drop was found to be only 1–2 mmHg for the parameters under consideration in this study. Since a pressure drop of this magnitude was found to have an insignificant effect on the results, the pressures in the cell and channel were assumed to be constant.

The sum of the cross-sectional areas of cell and channel

$$A \equiv A_e + A_c \tag{11}$$

is constant. As described previously [15], the cell wall is regarded as a flaccid membrane, moving in response to a pressure difference across it. The compliance function of such a membrane would have a sigmoidal shape characteristic of thin-walled tubes. If r is the fraction of wall area occupied by the channel, then typical compliance curves can be represented as hyperbolic tangents, with the general equation

$$r(x) = \frac{A_e(x)}{A} = \frac{r_{\max}}{1 + e^{-\xi[P_e(x) - P_c(x)]}} \tag{12}$$

where $r_{\max}$ is the limiting fractional area. The parameter ξ determines the stiffness of the wall; if ξ is large, the wall is flaccid, while if ξ is small, the wall is stiff, and responds less to changes in the transmural pressure difference. Since $P_e(x)$ and $P_c(x)$ do not vary significantly along the length of the channel, $r(x)$ also does not vary significantly along the length of the channel.

Under these assumptions we can replace Eqs. (5) and (6) with two first order equations that are sometimes more convenient for calculation

$$\frac{dC_e}{dx} \equiv b_e(x) \tag{13}$$

and

$$\frac{db_e}{dx} = \frac{[F_{ve}(x)\, b_e(x) - C_e(x)\, J_v(x) + J_s(x)]}{r A D_e}. \tag{14}$$

Similarly, from Eqs. (5)–(8) we derive for solute flow in the cell

$$\frac{dC_c}{dx} = b_c(x) \tag{15}$$

and

$$\frac{db_c}{dx} = \frac{1}{(1-r)\, A D_c} [F_{vc}(x)\, b_c(x) + C_c(x)\, J_v(x) - J_s(x)]. \tag{16}$$

We assume that the channel and cell terminate in uniform membranes. The boundary conditions are formulated using the equations of irreversible thermodynamics derived by Kedem and Katchalsky for homogeneous membranes. One important consideration is the behavior of the end geometry of the channel as the channel area changes. We tested two conditions at each end, conditions which we believe represent the limits of behavior. First, we assumed that the geometry of the end process remains constant for all conditions; second we assumed that the area (as reflected in the value of the permeability parameter) is directly proportional to the channel cross-sectional area. These options are incorporated in the boundary conditions through a modification of the channel permeabilities by the area ratio r at the ends of the channel.

At the tight junction, the equation for volume flow is

$$F_{ve}(0) = \left[\frac{\delta_t}{2} + (1-\delta_t)\frac{r}{r_{\max}}\right] L_{pt}[P_l - P_e + \sigma_t RT(C_e(0) - C_l)]. \tag{17}$$

The factor δ_t is either 0 or 1, depending on whether the membrane is to be variable or fixed, respectively. For the fixed case, the factor 1/2 is used so that the permeability will be equivalent to the variable case with the junction area at 50% of maximum. In this equation, L_{pt} is the area adjusted hydraulic permeability, with units $\mathrm{cm^3\,sec^{-1}\,mmHg^{-1}}$. The driving forces are the hydrostatic pressures, P_l and P_e, in the lumen and channel, respectively, and the osmotic pressures resulting from concentration $C_e(0)$ and C_l in the channel and tubule lumen, respectively. The reflection coefficient for NaCl is denoted by σ_t.

For solute flow across the tight junction, the conservation equation is

$$F_{ev}(0)\, C_e(0) - r\, AD_e b_e(0) = F_{ev}(0)\, \bar{C}_t(1-\sigma_t) + \left[\frac{\delta_t}{2} + (1-\delta_t)\frac{r}{r_{\max}}\right] H_{st}[C_l - C_e(0)]. \tag{18}$$

For $\bar{C}_t$, the average concentration within the junction, we use the arithmetic mean of the concentrations on each side, i.e.,

$$\bar{C}_t = (C_l + C_e(0))/2. \tag{19}$$

The solute permeability, H_{st}, is area adjusted, having units $\mathrm{cm}^3 \cdot \mathrm{sec}^{-1}$. A similar relation holds for the luminal cell membrane,

$$F_{vc}(0)\, C_c(0) - (1-r)\, AD_c b_c(0) = F_{vc}(0)\,(1-\sigma)\,(C_l + C_c(0))/2 + H_{sc}[C_l - C_c(0)]. \tag{20}$$

As for the tight junction, the arithmetic mean of the concentrations of the bathing solutions is used for average concentration within the luminal membrane. No area adjustment is included, since we assume that the area of the luminal membrane of the cell does not change.

Volume flow through the luminal cell membrane is given by

$$F_{vc}(0) = L_{pc}[P_l - P_c + RT\sigma_c(C_c(0) - C_c)] \tag{21}$$

where L_{pc} is the area adjusted permeability coefficient of the membrane. At the basal end of the channel ($x = L$), similar equations are written. For volume flow from channel to interstitium, the equation is

$$F_{ve}(L) = \left[\frac{\delta_b}{2} + (1-\delta_b)\frac{r}{r_{\max}}\right] L_{pb}[P_e - P_i + \Pi_i + RT\sigma_b(C_i - C_e(L))]. \tag{22}$$

This is similar to Eq. (17), but here the subscript b denotes the basement membrane, while the subscript i indicates interstitium, Π_i is protein oncotic pressure in the interstitial space. The basement membrane is assumed to be impermeable (or negligibly permeable) to protein.

For solute flow from channel to interstitium, the equation is

$$F_{ve}(L)\, C_e(L) - AD_e b_e(L) = F_{ve}(0)\,(1-\sigma_b)\,(C_e(L) + C_i)/2 + \left[\frac{\delta_b}{2} + (1-\delta_b)\frac{r}{r_{\max}}\right] H_{sb}[C_e(L) - C_i]. \tag{23}$$

We assume that the solute and hydraulic permeabilites of the basal cell membrane are sufficiently small that direct flow from cell to interstitium may be neglected. Thus, the boundary conditions for the basal cell membrane are

$$F_{vc}(1)=0 \tag{24}$$

and

$$F_{vc}(1)\, C_c(1)-(1-r)\, AD_c\, b_c(1)=0. \tag{25}$$

Equations (1)–(25) comprise the model. For these equations, the externally applied forces are tubule and interstitial pressures and solute concentrations. To simulate experimental conditions better, however, it is necessary to have a relation between peritubular capillary pressure and interstitial pressure, since in experimental investigations of transtubular flow the forces are applied via the capillary. If we assume that all of the tubular reabsorbate is reabsorbed by the capillaries, a conservation relation for volume flow across the capillary wall can be written. If we also assume that solute concentration in the interstitium C_i is the same as that in the plasma C_q, the driving force across the capillary wall consists of the combined hydrostatic and protein oncotic pressure differences between plasma and interstitium. In each unit area of capillary wall, the reabsorption rate is

$$Q=L_{pq}[P_i-\Pi_i)-(P_q-\Pi_q)]. \tag{26}$$

Here L_{pq} is the area adjusted permeability of the capillary wall, P_i and P_q are interstitial and capillary hydrostatic pressures, respectively, and Π_q and Π_i are protein oncotic pressures. We assume that the reflection coefficient for protein is 1.0. Since reflection coefficient for protein of the basement membrane is also assumed to be 1.0, we can express the combined hydrostatic and protein oncotic pressures by the simple terms P_I and P_{CAP}.

If we solve Eq. (26) for P_I, and also note that $F_{ve}(1)$ is equal to Q, we can substitute this expression in Eq. (22) to obtain

$$F_{ve}(1)\left[1+\frac{L_{pb}}{L_{pq}}\left(\frac{\delta_b}{2}+(1-\delta_b)\frac{r}{r_{\max}}\right)\right]=L_{pb}\left(\frac{\delta_b}{2}+(1-\delta_b)\frac{r}{r_{\max}}\right)\cdot[P_e-P_q+\Pi_q+RT\sigma_b(C_q-C_e(1))]. \tag{27}$$

Equations (1)–(27) comprise the boundary value problem of the model. The system was solved using a tested finite difference technique

[22] with ten spatial intervals. All computations were performed on a PDP-10 computer in double precision. The results are essentially identical with those obtained previously [15] using quasilinearization.

Normalization

The concentration was normalized to a concentration excess over isotonicity, by

$$\gamma = \frac{C - C_0}{C_0}.$$

The flow was normalized to a reference isotonic flow containing all the actively pumped solute. Thus,

$$\alpha(x) = \frac{F_v(x)}{\frac{1{,}000\, N_0}{C_0}}$$

where C_0 is in osmoles/liter, N_0 is in osmoles/sec, and F_v is in cm^3/sec.

Parameter Selection

The purpose of this study is not to determine the specific values of the membrane parameters of the system, but rather to determine the sensitivity of the system to each of the parameters, and thus to find which parameters are significant and which are not. Therefore, little attempt will be made to justify the values selected for the reference case; these values are based on experimental data where such is available, and on estimates where data are unavailable. Each parameter will be varied over a wide range, usually several orders of magnitude, to determine the system sensitivity. In this section will be discussed each of the parameter groups and any justification for the choice of the reference parameter.

Dimensions

The channel length was estimated to be approximately 25 μm. We assume that the change in channel cross-section area results from re-

orientation of the flaccid cell walls, and not from their stretching. When the channel is fully dilated, we assume that it will take the approximate shape of a circular cylinder, with circumference approximately three times the diameter. We estimate the diameter of the fully dilated channel to be 3 μm, hence the circumference is approximately 10 μm.

Whittembury [24] found the diameter of the cells to be approximately 6 μm. If the cells are circular, the cross-sectional area would be 28 μm^2; if, however, they assume some other shape (square, hexagon, etc.) the area would be larger. We selected a reference are slightly less than that of a square cell, namely, 34 μm^2.

Since the cell interior contains nontransportable material as well as water and electrolytes, it is clear that there is an upper limit to the dilation of the channels. A value of 0.15 was arbitrarily assumed for the maximum fractional epithelial area that can be occupied by channels at full dilation.

As discussed above, the channels will dilate or constrict as a function of the transmural hydrostatic pressure difference, with a compliance curve described by Eq. (12). The value of r/r_{max} varies between 0 and 1, and is equal to 0.5 when P_e equals P_c. The reference value, 0.083 $mmHg^{-1}$ of the compliance factor ξ was chosen such that when $P_e - P_c$ varies between -10 and $+10$ mmHg, the ratio r/r_{max} varies from 0.3 to 0.7.

Pumps

The solute pumps are assumed to be distributed over the length of the channel. At the present time, the distribution function is unknown. In this study, three distribution functions were considered: (i) The pump density decreases linearly from a maximum at the apical end to zero at the basal end; (ii) the pumps are uniformly distributed over the length; and (iii) the pump density increases linearly from zero at the apical end to a maximum at the basal end.

The rate of efflux from a tubule has been found to be approximately 1.8×10^{-6} ml/min/mm of tubule length at a transmural hydrostatic pressure difference of zero. Using the cell area given above, and a tubule luminal diameter of 40 μm, and assuming further that the transported fluid is isotonic (300 mosM), and that the lateral and basal cell walls are otherwise impermeable to solute, the transport rate from each cell is approximately 2.44×10^{-15} osmol/sec. Our earlier models [15] showed, however, that there could be a significant backleak of solute through the

tight junction. We therefore used, as a reference pumping rate, 2.8×10^{-15} osmol/sec.

Although the capability exists for putting in Michaelis-Menten kinetics, we deemed it inappropriate for this single-solute model. For these kinetics to show an appreciable effect, the solute concentration in the cell would have to be very low (i.e., much lower than isotonic); with only one solute, this condition would be accompanied by an unrealistically high cell hydrostatic pressure to maintain equilibrium.

Hydraulic Permeability

The lateral cell wall is assumed to be of fairly high hydraulic permeability; accordingly, a reference value of 5.07×10^{-7} cm/sec/mmHg was selected. The area adjusted value, obtained by multiplying this value by the circumference and length, is 1.27×10^{-12} cm^3/sec/mmHg. The permeabilities of the other membranes are normalized relative to this value. The basement membrane is assumed to be more permeable than the lateral cell wall; the reference permeability factor is 2.0. The tight junction is less permeable than the lateral wall; the initial reference factor is 0.2.

The apical cell wall is assumed to offer little resistance to the flow of water from the lumen to the cell; the initial reference permeability factor was 10.0. The basal cell wall is assumed to be impermeable to water, hence the factor is 0.0. The peritubular capillary is assumed to have the same permeability as the basement membrane, hence the factor is 2.0.

Solute Permeabilities

The membrane solute permeabilities are normalized by a reference channel solute permeability, which is the maximum channel area times the solute diffusion coefficient in the channel, divided by the channel length. The diffusion coefficient is taken to be the value for NaCl in dilute solution, which is approximately 1.5×10^{-5} cm^2/sec. This value is 3.06×10^{-10} cm^3/sec. This is the normalization constant used in all cases.

Initially, the channel wall was assumed to be impermeable to passive solute movement, so the permeability factor was 0.0. The basement membrane is assumed to be quite permeable, so the initial value of the factor was 2.0. This is not unreasonable, since if the permeability is

computed in the same way as for the channel, the smaller value of the thickness (or channel length) would yield a substantially larger value of permeability; the area is smaller, and the diffusion coefficient may also be smaller through the membrane.

The solute permeability of the tight junction is initially assumed, because of its presumably small cross-sectional area, to be smaller than that of the basement membrane. The initial estimate of the tight junction solute permeability factor is 0.2. The basal cell membrane is assumed impermeable to solute, hence the factor is 0.0; the apical membrane is assumed to be highly permeable, and the initial estimate of the permeability is 10.0.

Reflection Coefficients

The solute is assumed to exert its full osmotic force across the lateral cell wall, hence the reflection coefficient is 1.0. It is assumed that little sieving takes place through the basement membrane, so it is assigned a low reflection coefficient, 0.005. The tight junction on the other hand, is assumed to provide a significant impediment to convective solute flow, and an initial estimate of 0.7 was used for its reflection coefficient. The apical cell membrane, facing the lumen, is assumed to have a very small reflection coefficient, and an initial value of 0.001 was used. The basal cell membrane reflection coefficient is 1.0.

Diffusion Coefficients

Initially, it was assumed that solute diffuses in the channel and in the cell at approximately the same rate as in free solution. Hence, the values of D_e and D_c are both 1.5×10^{-5} cm^2/sec.

End Membrane Geometry

For the reference case, it was assumed that the cross-sectional area of the basement membrane opening varies in proportion to the channel cross-sectional area, and the cross-sectional area of the tight junction membrane remains constant for all channel conditions. Neither of these conditions can be reliably determined from micrographs; but either seems plausible.

In the numerical studies to be described, these parameters will be varied singly and in combination to determine how significant the value of each parameter is in determining the system output.

Results

Using the reference parameter set as set forth in the preceding section, the model was solved, yielding the flow and concentration profiles shown in Figs. 2 and 3. The concentrations in the lumen and in the interstitium are both isotonic, i.e., 300 mosmol, and the effective hydrostatic pressure difference between the lumen and the peritubular capillary is 25 mmHg, corresponding to a lumen hydrostatic pressure of 10 mmHg and a net capillary hydrostatic and protein oncotic pressure of −15 mmHg. The channel concentration is slightly hypotonic over its length, while the cell remains virtually isotonic. The channel pressure is −9.6 mmHg, and the cell pressure is 9.3 mmHg. The hydrostatic pressure in the interstitium is −14.2 mmHg. The pressure difference across the cell wall results in a channel cross-sectional area 0.0258 of the unit cell area.

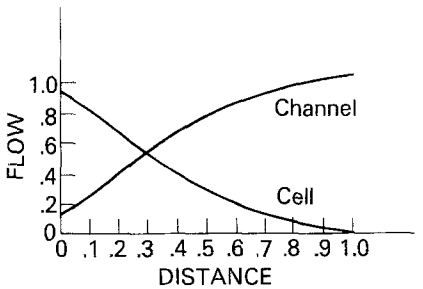

Fig. 2. Flow profiles in channel and cell. All parameters have their reference values, the luminal hydrostatic pressure is 10 mmHg, and the combined peritubular capillary oncotic and hydrostatic pressure is −15 mmHg

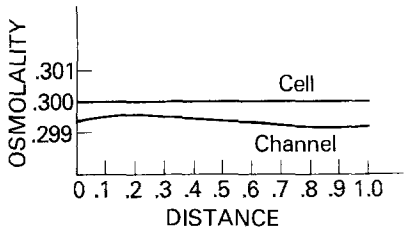

Fig. 3. Concentration profiles for channel and cell. All parameters and independent variables have their reference values

At the tight junction, the channel flow is 0.135, which is approximately 12% of the emergent flow. Because of the high reflection coefficient of the tight junction, a high sieving occurs, and the entering fluid is significantly hypotonic, having an osmolality of 0.107. For the first interval of the channel, then, the fluid is hypotonic; the fluid entering through the wall (J_v) in this interval, including the solute pumped, is approximately 0.74 osmolar, and thus the channel fluid becomes less hypotonic. By the time the channel fluid reaches the point 0.1 in the channel, the flow osmolality (defined as solute flow divided by volume flow) is 0.285.

Figure 4 shows the transmural volume flow as a function of distance along the channel. As can be seen from Eq. (9), net water flow into the channel results from the algebraic sum of hydrostatic and osmotic forces; thus it can be split into hydrostatic and osmotic components, which may be opposite in direction. Since the hydrostatic pressures in the channel and in the cell remain constant, the hydrostatically induced flow is constant. The osmotic flow on the other hand, shows a minimum at about 0.2. This is due to the slight rise in the channel osmolality at this point, which results, in turn, from the large amount of solute pumped in near the apical end of the channel.

It is important to note that the magnitudes of the flows due to hydrostatic and osmotic components are of the same order of magnitude,

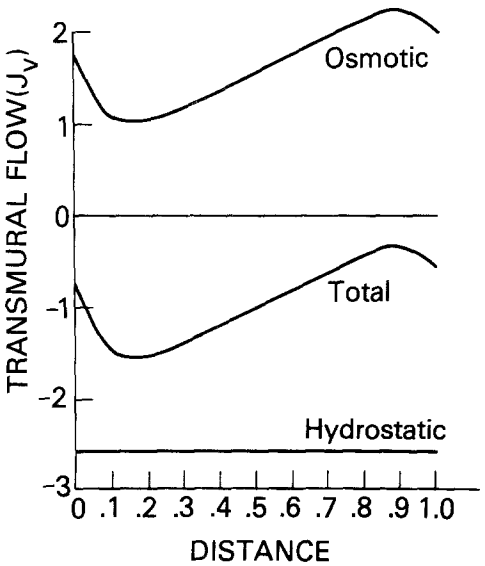

Fig. 4. Transmural flow (J_v) profile. All parameters and independent variables have their reference values

with the hydrostatic term opposite in sign to but greater in magnitude than the osmotic term. Thus, the direction of flow is determined by the hydrostatic pressure.

The reabsorbate is, in this case, slightly hypotonic, having an osmolality of 0.2901. Although almost no sieving occurs, the emergent osmolality is not equal to the channel concentration at the basement membrane due to diffusion into the channel from the interstitium. Thus, convection and diffusion are in opposite directions.

One of the objectives of this study was to determine the effect of changes in the hydrostatic pressure difference across the epithelium on transepithelial fluid flow. Green, Windhager, and Giebisch [13] showed that, over a wide range of oncotic pressure differences, the transepithelial flow responds in a nearly linear fashion. In our study, the effective capillary pressure was kept constant at -15 mmHg, while the luminal pressure was set at 0, 10, and 20 mmHg. Figure 5 shows the flow as a function of pressure, and Fig. 6 shows the emergent osmolality as a function of pressure.

The data of Fig. 5 show that changes in the transepithelial pressure cause a change in flow, although the slope is not linear. The fractional increase in flow when pressure changes from 15 to 25 mmHg is approximately 0.02.

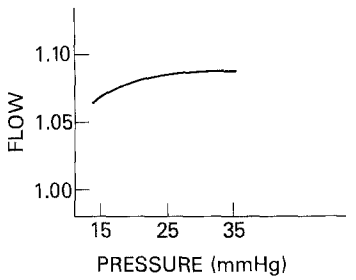

Fig. 5. Effect of transtubular hydrostatic pressure difference on flow through channel

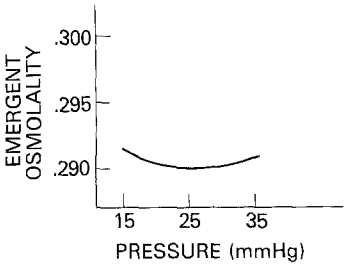

Fig. 6. Effect of transtubular hydrostatic pressure difference on osmolality of reabsorbate

The emergent osmolality is approximately 0.291 over the range of pressure considered. This is significantly hypotonic; however, since these results reflect only the reference parameters, this is not indicative of the actual system performance. In the following section will be discussed the effects of changes in the parameters on the system operation.

Parameter Sensitivity

Each parameter value was varied over a range one to 2 orders of magnitude on either side of its reference value. Because of the nonlinearity of the model, quantitative effects are highly dependent on the specific values chosen for the other parameters; therefore, only gross effects will be discussed in this section.

Tight Junction: The tight junction parameters (hydraulic permeability, solute permeability and reflection coefficient) have little effect on emergent osmolality or hydrostatic pressures in the system so long as the wall permeability is sufficiently high to allow equilibration. However, the sensitivity of flow to changes in transepithelial hydrostatic pressure is significantly affected by the values of these parameters. An increase in H_{st} or a decrease in σ_t will result in an increase in the pressure sensitivity, so long as there is some volume flow across the tight junction.

Basement Membrane

The values of the basement membrane parameters have a significant effect on all aspects of the system performance: sensitivity of flow to changes in transepithelial pressure, emergent osmolality, and pressure and concentration in the channel. In general, a parameter change that tends to restrict flow out of the channel will increase the emergent osmolality and decrease the flow.

Channel Wall

If the channel wall permeability decreases such that equilibration does not occur, both the channel fluid and the emergent fluid will be hypertonic.

It was originally assumed that the solute permeability of the wall is zero. If the wall is made permeable to solute, additional solute moves into the

hypotonic channel; the added solute draws additional water from cell to channel, and the net result is that the flow increases, as does the sensitivity of flow to transepithelial pressure. The effect on emergent osmolality is minimal.

Luminal Cell Membrane

The luminal cell membrane was assumed to be highly permeable to both fluid and solute, with a very low reflection coefficient. No changes in the system operation are observed when this membrane is made more permeable; however, when the permeability is decreased, the cell pressure drops in order to maintain the required flow. It is unreasonable to allow these permeabilities to fall to a point where the cell pressure becomes physiologically unrealizable. This situation cannot be properly analyzed for a single solute system. For a multisolute system, the solute permeabilities can be varied individually, such that sodium can be restricted without causing a drop in cell pressure.

Geometry

Generally, changing a parameter to decrease the channel volume results in an increased emergent fluid osmolality. The reference cell has a compliant wall. If the wall is assumed to be stiff, and the channel area constant, the flow may become more sensitive to changes in the transepithelial pressure difference. The emergent osmolality is probably also dependent on the compliance.

Solute Pumps

The behavior of the system is highly dependent on the pumping rate. When the pumping rate is low, the hydrostatic pressures are more influential. As the pumping rate increases, the osmotic pressures in the system become dominant and hydrostatic pressures, both outside the epithelium and in the cell and channel, become less important.

The pump distribution has only a minor influence on the system. In general, however, the more dense the pumps are at the basal end, the higher is the tonicity of the emergent fluid.

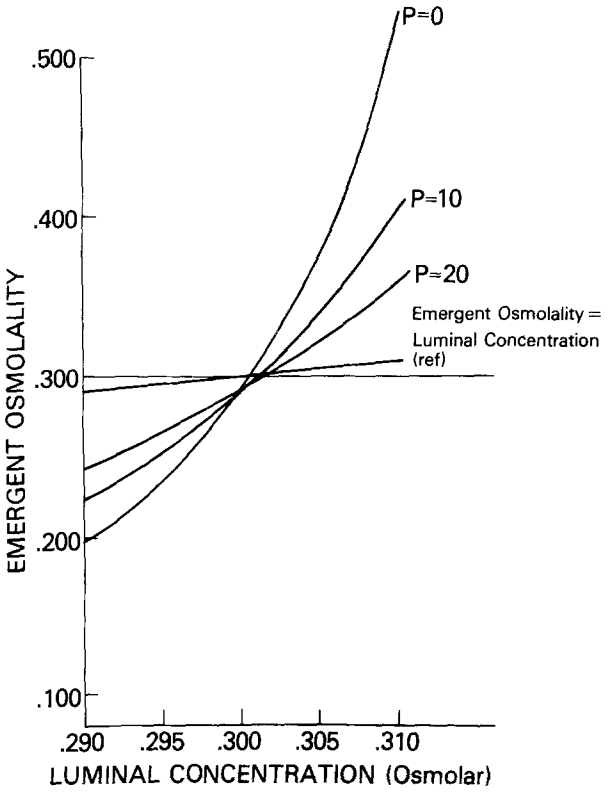

Fig. 7. Effect of luminal concentration on emergent osmolality for various values of luminal hydrostatic pressure. Peritubular capillary pressure is −15 mmHg in all cases

Luminal Concentration

In Fig. 7 is shown the effect of varying luminal concentration on the osmolality of the reabsorbed fluid. It can be seen that the osmolality of the fluid emerging from the channel is critically dependent on the concentration of the luminal fluid, varying from 0.500 M to 0.200 M over a range of luminal concentration of 0.020 M. The slope characteristic depends on the luminal hydrostatic pressure, but in all simulations decreased monotonically as luminal concentration decreased.

Discussion

The sensitivities discussed above are contingent on the fact that the remaining parameters have their reference values. By adjusting other parameters, some individual sensitivities may be changed or even reversed. Thus, the results may have only a restricted validity.

In testing each of the parameters, one result that emerged consistently was the relative constancy of the concentrations in the channel and the cell. These values seldom changed more than 1 mosmol when a parameter was altered by an order of magnitude. When changes occurred, they were compensated by changes in the hydrostatic pressures in the cell and channel. The hydrostatic pressure, then, acts to maintain a relatively constant concentration throughout the epithelial layer.

The numerical results showed so little variation in concentration over the length of the channel and the cell as to suggest that these compartments are well enough mixed to be approximated by a simpler compartment model. Such a model was developed, and the results were found to be essentially the same as those obtained using the differential equation model.

The most significant feature to emerge from this study is the controlling influence of luminal osmolality on the osmolality of the fluid absorbed from the proximal tubule (the emergent osmolality). The absorption characteristics shown in Fig. 7 result in the rapid equilibration of proximal tubule absorbate and luminal contents at near isotonicity, by a general mechanism we have discussed in detail previously [21].

The change in the osmolality of proximal tubule fluid with distance along the tubule is easily derived. Under the assumption that axial diffusive flow is negligible relative to axial convective flow, the equation for conservation of axial solute flow is

$$d(F_{vl}\, C_l)/dx = -J_{sl} \tag{28}$$

and for volume

$$dF_{vl}/dx = -J_{vl} \tag{29}$$

where F_{vl} is total axial volume flow along the proximal tubule, C_l is luminal concentration, assumed radially constant, J_{sl} is transmural solute flow and J_{vl} is transmural volume flow per unit length of proximal tubule (J_{vl} equals the product of $F_{ve}(1)$ by the number of channels per unit length). On differentiating Eq. (28) and substituting Eq. (29) we obtain

$$dC_l/dx = [-J_{sl} + J_{vl}\, C_l]/F_{vl} \tag{30}$$

which can be rewritten

$$\frac{dC_l}{dx} = \frac{J_{sl}}{F_{vl}}\left[\frac{C_l}{C_A} - 1\right] \tag{31}$$

where the osmolality of the absorbate $C_A \equiv J_{sl}/J_{vl}$.

If J_{sl}/F_{vl} is positive, then concentration in the direction of flow will decrease if $C_A > C$ and will increase $C_A < C$. Thus, after glomerular filtration, proximal tubule fluid will approach the equilibrium condition $C_A = C_l$. This equilibrium value is found by the intersection of the curves for emergent osmolality as a function of C_l with the identity line $C_l = C_A$. For Fig. 7 the intersection points are between 0.3005 and 0.3015. In the absence of a pressure gradient from lumen to capillary, the equilibration values would be slightly hypotonic.

The rapidity of equilibration is easily estimated. Normalizing distance along the tubule, and multiplying both sides of Eq. (31) by $1/C_l$, we obtain

$$\frac{dC_l}{C_l dx'} = \frac{J_{sl} L}{F_{vl} C_l}\left[\frac{C_l}{C_A} - 1\right] \tag{32}$$

where L is the length of the tubule and $x' = x/L$. Letting

$$C_l = C_E + \Delta C, \tag{33}$$

$$C_A = C_E + \left(\frac{\partial C_A}{\partial \Delta C}\right)_{C_A = C_E} \Delta C, \tag{34}$$

$$= C_E + \beta \Delta C, \tag{35}$$

where C_E denotes the equilibrium concentration, and $\beta = (\partial C_A/\partial \Delta C)_{C_A = C_E}$ is the slope characteristic of the reabsorbate, we find

$$\frac{d\Delta C}{dx'} = f C_l \left[\frac{(1-\beta)\Delta C}{C_E + \beta \Delta C}\right]. \tag{36}$$

If f, which approximates fractional solute absorption out of proximal tubule, is held constant (since $C_l \cong C_E$ is approximately constant) this equation can be integrated to give

$$\frac{1}{1-\beta} \ln \frac{\Delta C}{(\Delta C)_{x=0}} + \frac{\beta}{1-\beta}\left[\frac{\Delta C - \Delta C(0)}{C_E}\right] = f x' \tag{37}$$

or approximately

$$\Delta C = (\Delta C)_{x=0} \exp[(1-\beta) f x']. \tag{38}$$

For the curves of Fig. 7, the slope β is a number between 5 and 20. Thus, taking fractional PT absorption to be 0.5, we find $C_l - C_E$ drops to 1/2 its initial value in between 0.05 and 0.5 of normalized PT length. Figure 8 shows a typical profile for a tube of nominal length 1 cm.

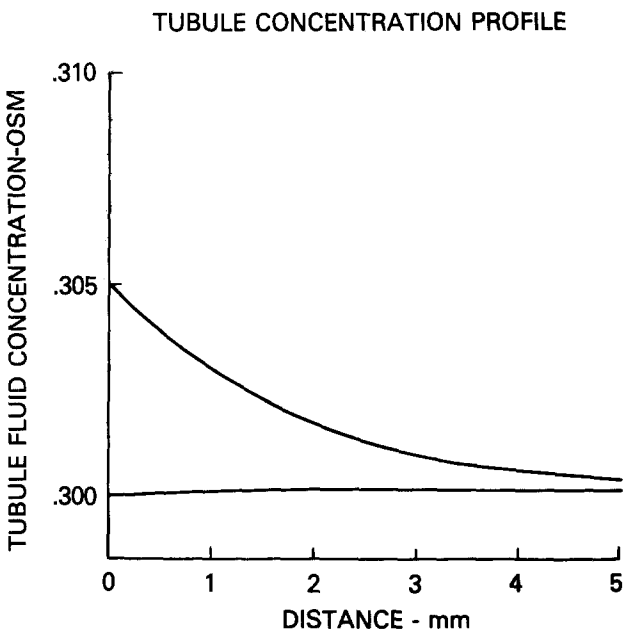

Fig. 8. Typical concentration profile for a tubule of nominal length, 1 cm

The view of *PT* absorption suggested to us by the model differs sharply from the traditional view. Instead of "isotonic" absorption we find that the steep slope characteristic of the osmolality of the absorbate as a function of luminal osmolality causes:

1) luminal fluid and absorbate to equilibrate at quasi-iso-osmolality;
2) this equilibration to occur in a short fraction of *PT* length.

References

1. Boulpaep, E.L. 1972. Permeability changes of the proximal tubule of *Necturus* during saline loading. *Am. J. Physiol.* **222**:517
2. Brenner, B.M., Falchuk, K.H., Keimowitz, R.I., Berliner, R.W. 1969. The relationships between peritubular capillary protein concentration and fluid reabsorption by the proximal tubule. *J. Clin. Invest.* **48**:1519
3. Brenner, B.M., Galla, J.H. 1971. Influence of post-glomerular hematocrit and protein concentration in rat nephron fluid transfer. *Am. J. Physiol.* **220**:148
4. Brenner, B.M., Troy, J.L. 1971. Post-glomerular vascular protein concentration: Evidence for a causal role in governing fluid reabsorption and glomerulotubular balance by the renal proximal tubule. *J. Clin. Invest.* **50**:336
5. Burg, M.B., Grantham, J.J. 1971. Ion movements in renal tubules. *In:* Membranes and Ion Transport. E.E. Bittar, Editor. Vol. 3, p. 49. Wiley-Interscience, London

6. Burg, M.B., Orloff, J. 1968. Control of fluid absorption in the renal proximal tubule. *J. Clin. Invest.* **47**:2016
7. Diamond, J.M. 1974. Tight and leaky junction of epithelia: A perspective on kisses in the dark. *Fed. Proc.* **33**:2220
8. Diamond, J., Bossert, W.H. 1967. Standing gradient osmotic flow. A mechanism for coupling of water and solute transport in epithelia. *J. Gen. Physiol.* **50**:2061
9. Frizzell, R.A., Schultz, S.G. 1972. Ionic conductances of extracellular shunt pathway in rabbit ileum. Influence of shunt on transmural sodium transport and electrical potential differences. *J. Gen. Physiol.* **59**:318
10. Frömter, E. 1972. The route of passive ion movement through the epithelium of *Necturas* gallbladder. *J. Membrane Biol.* **8**:259
11. Frömter, E., Diamond, J. 1972. Route of passive ion permeability variation in epithelia. *Nature, New Biol.* **235**:9
12. Gertz, K.H. 1973. Transtubulare Natriumchloridflüsse und Permeabilität für Nichtelektrolyte im proximalen und distalen Convolute der Rattenniere. *Pfluegers Archiv.* **276**:336
13. Green, R., Windhager, E.E., Giebisch, G. 1974. Protein oncotic pressure effects on proximal tubular fluid movement in the rat. *Am. J. Physiol.* **226**:265
14. Humphreys, M.H., Earley, L.E. 1971. The mechanism of decreased intestinal sodium and water reabsorption after acute volume expansion in the rat. *J. Clin. Invest.* **50**:2355
15. Huss, R.E., Marsh, D.J. 1975. A model of NaCl and water flow through paracellular pathways of renal proximal tubules. *J. Membrane Biol.* **23**:305
16. Huss, R.E., Stephenson, J.L., Marsh, D.J. 1976. Mathematical model of proximal tubule solute and water transport. *(Abstr.) Physiologist* **19**:236
17. Kaye, G.I., Wheeler, H.O., Whitlock, R.T., Lane, N. 1966. Fluid transport in the rabbit gall bladder. A combined physiological and electron microscope study. *J. Cell Biol.*
18. Martino, J.A., Earley, L.E. 1967. Demonstration of a role of physical factors as determinants of the natriuretic response to volume expansion. *J. Clin. Invest.* **46**:1963
19. Seely, J.F. 1973. Effects of peritubular oncotic pressure on rat proximal tubule electrical resistance. *Kidney Int.* **4**:28
20. Spitzer, A., Windhager, E.E. 1970. Effect of peritubular oncotic pressure changes on proximal tubular fluid reabsorption. *Am. J. Physiol.* **218**:1188
21. Stephenson, J.L. 1973. The mathematical theory of renal function. *In:* Engineering Principles in Physiology. Vol. 2, pp. 283–320. J.H.V. Brown and D.S. Gann, editors. Academic Press, New York—London
22. Stephenson, J.L., Tewarson, R.P., Mejia, R. 1974. Quantitative analysis of mass and energy balance in nonideal models of the renal counterflow system. *Proc. Nat. Acad. Sci.* USA **71**:1618
23. Tormey, J.McD., Diamond, J.M. 1967. The ultrastructural route of fluid transport in rabbit gall bladder. *J. Gen. Physiol.* **50**:2031
24. Whittembury, G. 1967. Sobre los mecanismos de absorción en el tubo proximal del riñón. *Acta Cient. Venezolana (Suppl.)* **3**:71